NASA TN D-1714

NASA TN D-1714

TECHNICAL NOTE

D-1714

PORTABLE INTEGRATING SPHERE FOR MONITORING REFLECTANCE OF SPACECRAFT COATINGS

W. B. Fussell and J. J. Triolo

Goddard Space Flight Center
Greenbelt, Maryland

and

F. A. Jerozal

Continental Technical Service, Inc.
Silver Spring, Maryland

NATIONAL AERONAUTICS AND SPACE ADMINISTRATION

WASHINGTON

April 1963

Cable-1

PORTABLE INTEGRATING SPHERE FOR MONITORING REFLECTANCE OF SPACECRAFT COATINGS

by
W. B. Fussell and J. J. Triolo
Goddard Space Flight Center
and
F. A. Jerozal
Continental Technical Service, Inc.

SUMMARY

In the thermal design of spacecraft, the input term in the radiation balance equation for a space vehicle in free space—removed from significant earth radiation—is directly proportional to the solar absorptivity of the illuminated portion of the vehicle. For opaque spacecraft coatings, incident solar radiation which is not absorbed must be reflected; thus, the solar absorptivity of such coatings can be computed from spectrally resolved total reflectance measurements. It is shown that total reflectance data at wavelengths between 0.27 and 1.65μ enable the solar absorptivities of common spacecraft coatings to be estimated to within approximately ± 20 percent or better.

An integrating sphere is the most convenient device for measuring the total reflectance of opaque coatings of different degrees of curvature, specularity, and diffusivity. A portable, 8-lb, single-beam, 6-inch diameter integrating sphere reflectometer has been designed and fabricated at the GSFC and has been used extensively to detect changes in the solar absorptivity of spacecraft coatings due to environmental testing, ageing, or contamination.

CONTENTS

PORTABLE INTEGRATING SPHERE FOR MONITORING REFLECTANCE OF SPACECRAFT COATINGS

by
W. B. Fussell and J. J. Triolo
Goddard Space Flight Center
and
F. A. Jerozal
Continental Technical Service, Inc.

INTRODUCTION

In the thermal design of spacecraft (Reference 1), the input term in the radiation balance equation for a space vehicle in free space (removed from significant earth radiation) is directly proportional to the average solar absorptance of the vehicle's illuminated portion. The output term in the radiation balance equation, neglecting internally generated power, is directly proportional to the average thermal emittance of the vehicle's total exterior surface. Therefore, with the above approximation, its equilibrium temperature is proportional to $(\bar{a}/\bar{e})^{0.25}$, where $\bar{a}$ = average solar absorptance, and $\bar{e}$ = average thermal emittance. In a space vehicle whose outer surface is composed of several materials, $\bar{a}$ is computed by summing the individual terms for each material illuminated by the sun. Each term is the product of its solar absorptance (which, in general, depends upon the angle of incidence of the sun's rays on each element of surface) multiplied by the fraction of the total projected area normal to the material's direction of illumination.

Thus it is highly desirable to measure at least the normal solar absorptance of small areas of a vehicle's surface. For opaque spacecraft coatings, the incident solar radiation which is not absorbed must be reflected. The solar absorptance of such coatings can therefore be computed from spectrally resolved total reflectance measurements. Or, if a solar simulator (a terrestrial light source whose spectral distribution matches that of the sun from the thermal design point of view) is available, a total reflectometer can be devised which will yield the solar absorptance from nonspectrally resolved data.

Although it is desirable to obtain a complete curve of a given coating's total reflectance as a function of wavelength from at least 0.3 to 2.5μ, suitable assumptions about—or prior knowledge of—the general nature of the absorptance spectrum often make data at a few selected wavelengths very helpful and permit an approximate estimate of the solar absorptance to be made. In most cases the coating material is known and the problem is one of detecting small changes in the solar absorptance due to contamination, that is, to surface deterioration caused by handling, corrosion, tarnishing, or environmental testing.

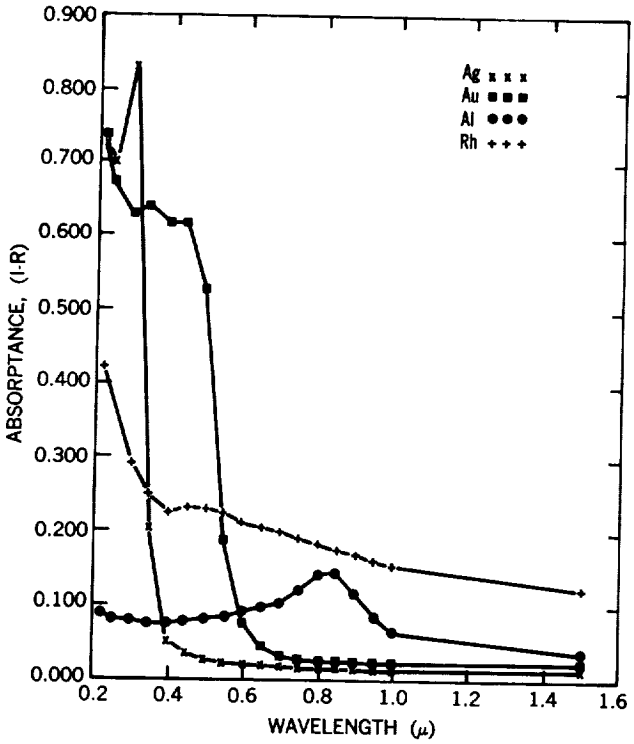

Figure 1—Absorptance of Al, Ag, Au, and Rh versus wavelength (data from Reference 2).

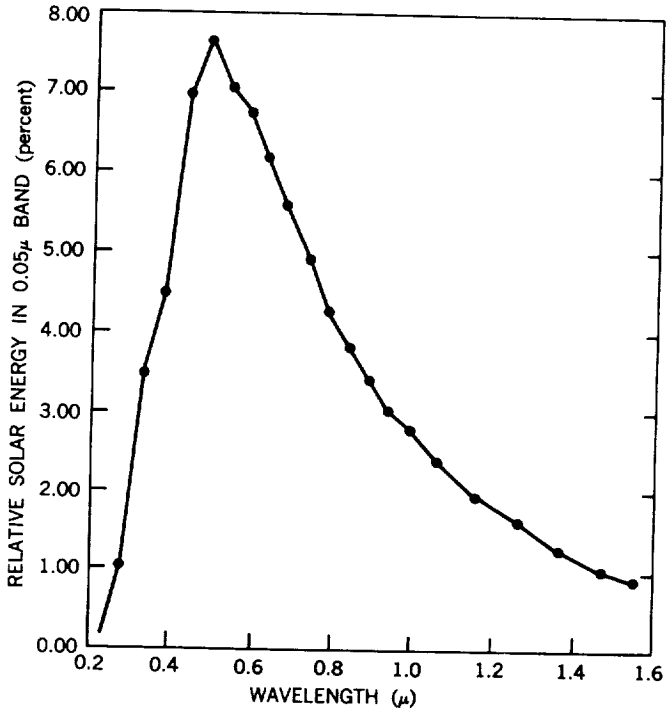

Figure 2—Extra-terrestrial solar spectrum versus wavelength (data from Reference 3).

Metal surfaces are usually more sensitive to contamination and surface condition than paints. This is partly due to their low absorptance when clean, vacuum-deposited, surfaces are measured. For example the solar absorptances of some common metals are: aluminum, $\bar{a}$ = 7.78%; gold, $\bar{a}$ = 19.25%; silver, $\bar{a}$ = 4.9%; and rhodium, $\bar{a}$ = 18.25% (Reference 2). It is especially important, therefore, that metallic spacecraft coatings be checked frequently for increased values of solar absorptance due to surface deterioration. It is of interest at this point to note that 80% of the absorbed solar energy lies between 0.27 and 0.89μ for silver, and between 0.41 and 1.13μ for aluminum. In both cases, 10 percent of the absorbed energy occurs at shorter wavelengths than the short wave limits, and another 10 percent occurs at longer wavelengths than the long wave limits. For a perfect black paint, the 80 percent limits—as defined above—are 0.41 and 4.65μ. It is felt that measurements of absorptance between the 80 percent limits for any coating should enable the solar absorptance of the coating to be estimated to better than 20 percent of its true value. Figure 1 presents the absorptance spectra of the four metals previously mentioned (Reference 2).* Silver and aluminum represent the opposite extremes with respect to the wavelengths of the dominant regions of absorption. For comparison, the solar extra-terrestrial spectrum, derived from Johnson's data (Reference 3), is displayed in Figure 2. Figures 3 and 4 present the average absorptance for aluminum, gold, silver, and rhodium, multiplied by the percent of solar energy increments for small bandwidths, starting (except for silver, where 0.25μ is the initial point) at 0.30μ and running out past 5μ and integrated from

*The data is that given by Dr. Hass of ERDL, Fort Belvoir, in the A.I.P. Handbook.

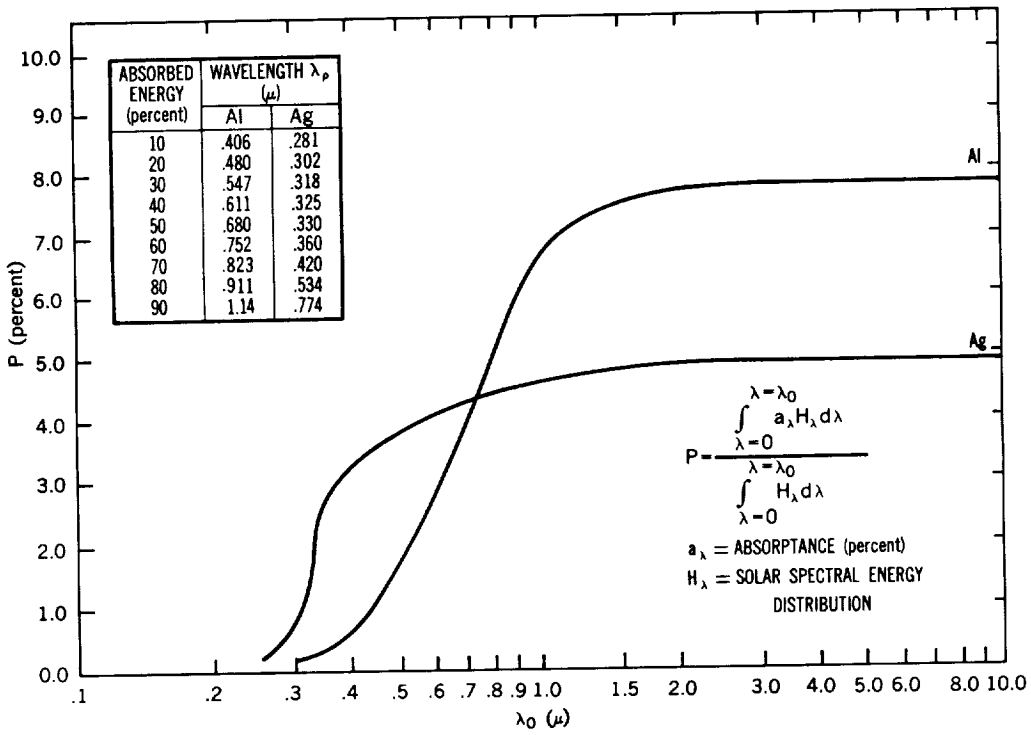

Figure 3—Absorbed solar energy from a nominal $\lambda = 0$ to $\lambda = \lambda_0$, versus λ_0 for aluminum and silver.

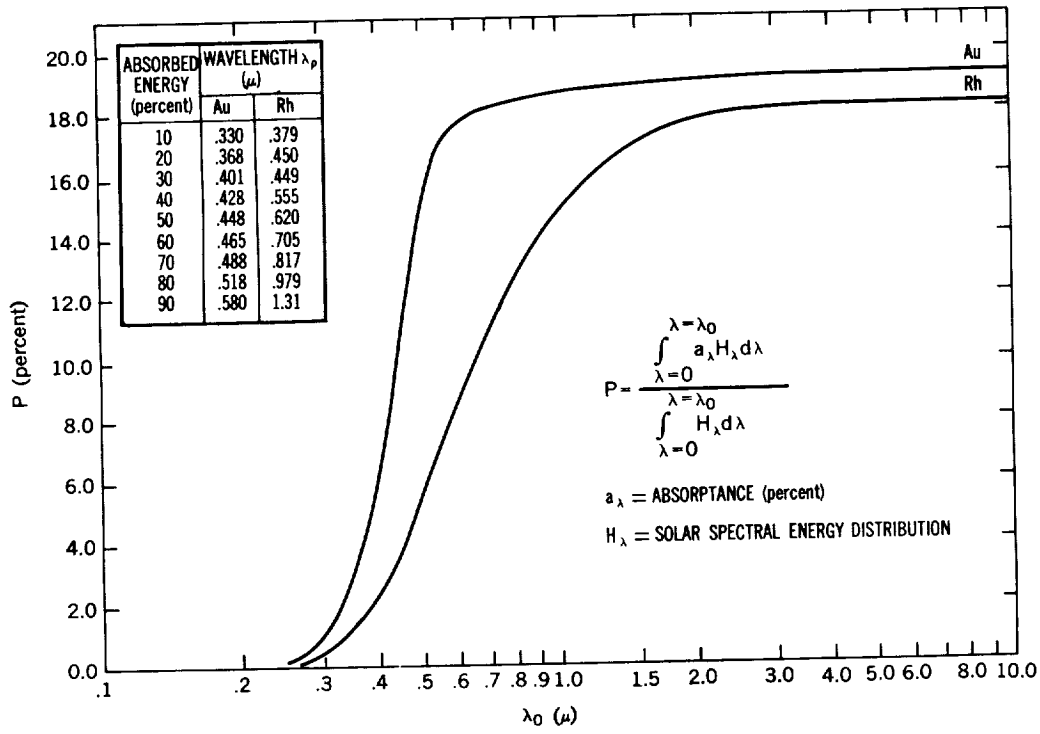

Figure 4—Absorbed solar energy from a nominal $\lambda = 0$ to $\lambda = \lambda_0$, versus λ_0 for gold and rhodium.

a nominal $\lambda = 0$ to $\lambda = \lambda_0$ versus λ_0, the wavelength. These figures give a good picture of the dominant wavelength interval within which the major portion of the sun's energy is absorbed by each of these metals.

THE INTEGRATING SPHERE COATINGS MONITOR AND ITS PURPOSE

Spacecraft surfaces often have various degrees of curvature and surface roughness. An integrating sphere is a convenient device for measuring the total reflectance of such surfaces, since it collects nearly all the reflected light—independent of whether the light is diffusely or specularly reflected—and is independent of the radii of curvature of the surfaces, provided the radii are larger than a certain minimum radius set by the geometry of the sphere. Figure 5 presents a cross-section view of a 6-inch diameter, single-beam, integrating sphere fabricated recently at Goddard Space Flight

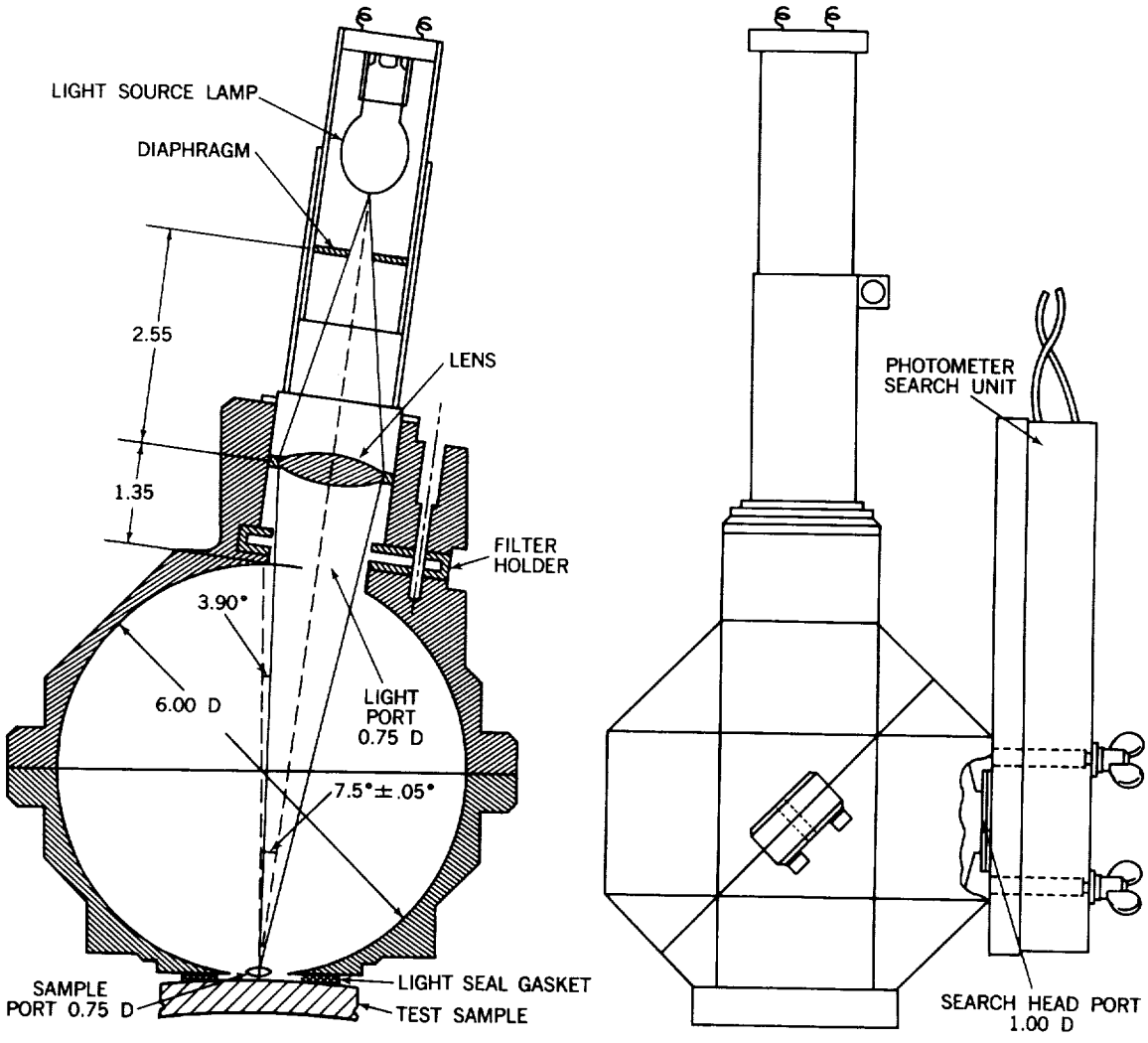

Figure 5—Cross-section of the integrating sphere with all dimensions in inches.

Center for monitoring the solar absorptance of spacecraft coatings. The interior of the sphere is coated with the barium sulfate paint described by Middleton and Sanders (Reference 4). As Figure 5 shows, light from the lamp goes through the small aperture.* The aperture is focused by the glass lens on the sample which is pressed close to the exterior of the sample port. Light reflected from the sample is collected by the sphere (in diffusely reflecting materials, a small fraction of the light is lost out the light source port) and produces a uniform illumination on the inner wall of the sphere viewed by the photomultiplier detector. A slot is available in the light source housing into which standard 2×2 in. square interference, or other, filters can be inserted. The lamp used in the light source, a General Electric Co. No. 1493 Microscope Illuminator Lamp, is rated at 6.5 v and 2.75 amp.

It has been found by experiment that the luminous intensity of a new lamp is not steady; however, if the lamp is aged for an hour at its rated voltage and current, it is stable thereafter (Reference 5). It was found that satisfactory stability of the light output from the lamp could only be achieved with an ultra-stabilized power supply for the lamp. It can easily be shown that the light output from the lamp (considered as a grey body) over a narrow wavelength interval is a very sensitive function of the temperature. For example, for a lamp having a color temperature of 2800° Kelvin, the radiant output at a wavelength of 5000A varies as the equivalent of the 10th power of the temperature:

$$\frac{J_\lambda(T+\Delta T)}{J_\lambda(T)} = 1 + \frac{\Delta T}{T}\frac{C_2}{\lambda T} = 1 + 10\frac{\Delta T}{T} ,$$

where

J_λ = radiant output per unit wavelength, bandwidth and unit surface area,

T = absolute temperature of the lamp (°K),

C_2 = 1.438 cm-°K,

λ = wavelength (cm).

After some experimentation, a Model 808 AX Power Supply was found satisfactory.† This is a chopper-stabilized, regulated power supply which regulates to better than 0.01 percent (or 1 mv) for both line and load (Reference 5). The photomultiplier tube, its housing, and its associated amplifier, power supply, and output indicating meters are part of a 520-M Photometer.‡ Photomultiplier tubes having S-1, S-4, S-5, and S-11 spectral sensitivity cathodes are available as accessories for this equipment. It was also found necessary to use a Sola Model CV-1 Constant Voltage Transformer (500 VA-115v) in the power line for the 520-M Photometer.§ This is a harmonic-free, static magnetic voltage regulator (Reference 5). The 520-M has a small, internal magnetic regulator, but this proved insufficient. Combined with the ultra-stable light source power supply, the Model CV-1 magnetic

*A number of apertures are available, in sizes ranging from 1/16 to 3/8 in. diameter. Here a collector lens between the lamp and the aperture would be desirable to increase the amount of light collected from the lamp.
†Made by Harrison Laboratories, Inc., Berkeley Heights, N. J.
‡Made by the Photovolt Corporation, 95 Madison Avenue, N. Y. 16, N. Y.
§Obtained from Allied Radio Corp., Chicago 80, Ill.

voltage regulator gave a highly stable output. Short-term fluctuations were less than ±0.5 percent, and long-term drift was less than 8 percent per day. Figure 6 displays the complete integrating sphere coatings-monitor-apparatus. The integrating sphere is at left; attached to the right side of the sphere is the photomultiplier housing. On top of the power supply console is the photovolt photometer amplifier, showing the large meter which indicates the light level striking the photomultiplier tube. (The photometer has provision for attaching a recorder. As yet, however, a recorder has not been used with this equipment.) Detailed operating instructions and electronics alignment procedures are given in Reference 5. Figure 7 shows the rear storage compartments of the power supply console with the integrating sphere and output indicators in position. The total weight of the integrating sphere with the detector housing and light source attached is about 8 lbs.

The operating procedure for the sphere will be presented briefly:

1. The lamp and the photomultiplier supply are turned on and the equipment allowed to warm up for one-half hour.

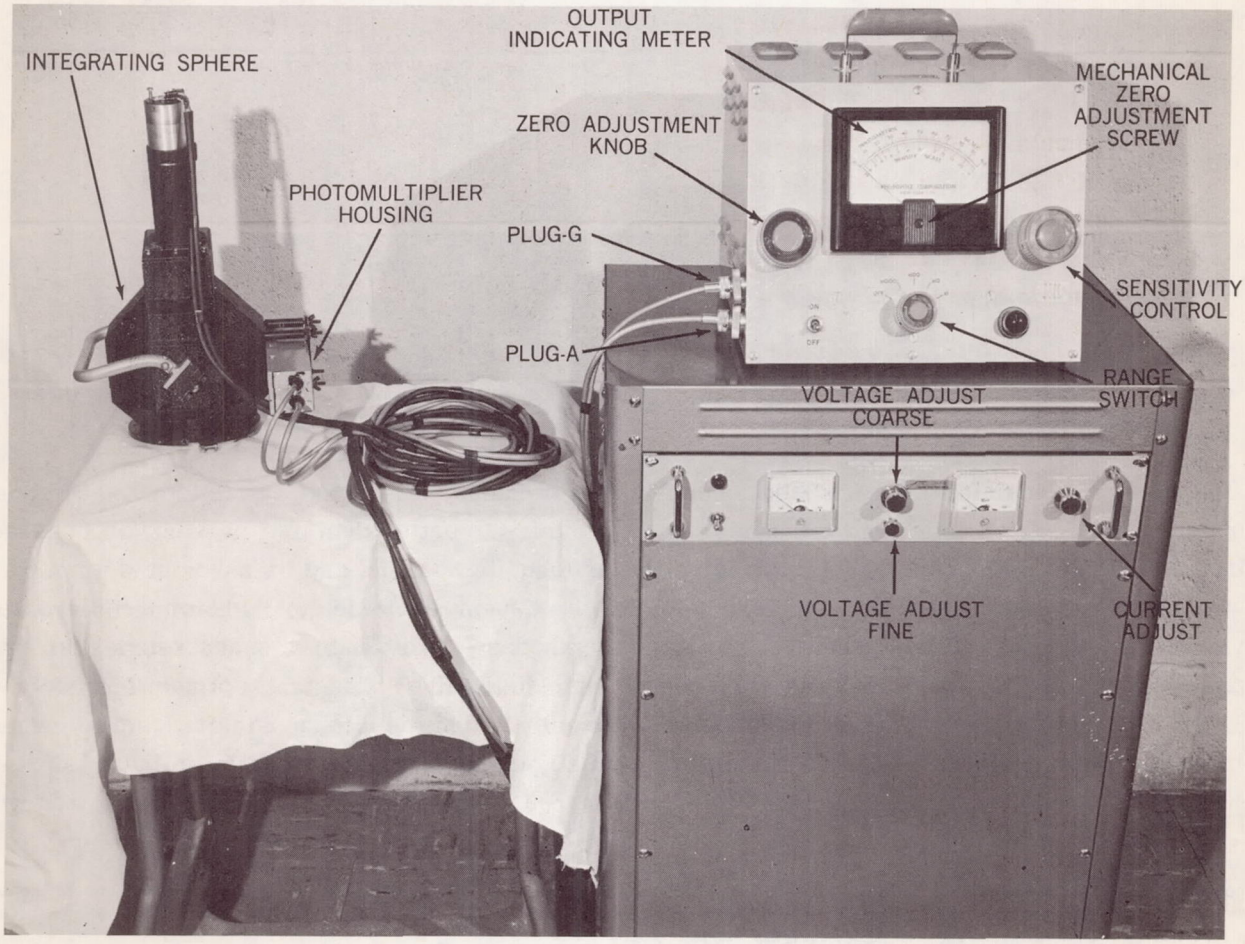

Figure 6—Reflectance monitor panel components.

2. An opaque blank is placed in the filter slot and the output meter checked for zero on all ranges (the sample port must also be blocked off during this check).

3. With the high voltage off the photomultiplier dynodes (to avoid damage to the photomultiplier by excessive current, due to stray light leaking into the sphere through the sample port) a known standard of specular reflectance, for example vacuum deposited gold or aluminum on glass, is placed over the sample port if the test sample is also specular, or nearly so. If the test sample is highly diffuse, a reference sample coated with a thick layer (at least 6 mm) of MgO smoke should be used. The substrate of the sample should be a polished metal surface to secure a reflectance near that given in the literature for MgO (Reference 6).

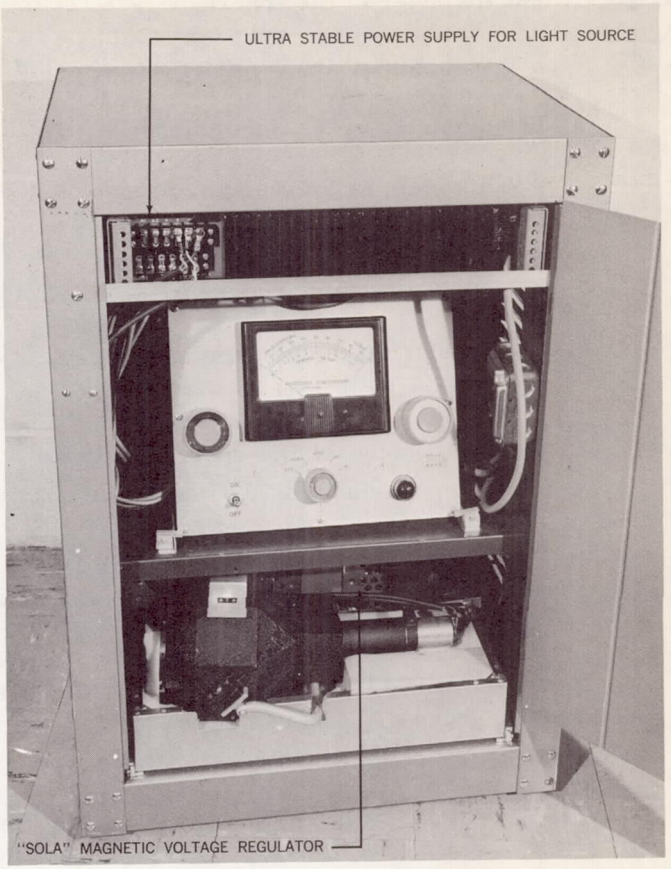

Figure 7—Reflectance monitor storage compartment.

4. After the reflectance standard is securely pressed against the light seal gasket so that no stray light enters the sphere and firmly enough so that the surface of the standard is within at least 1/8 in. of the sample port, the photomultiplier voltage is turned on, and the sensitivity of the output meter is adjusted until the meter reads a convenient value (for example, 80) near the high end of the scale. The reading for the standard is recorded, and the high voltage to the photomultiplier turned off again.

5. The reflectance standard is now removed from the sample port and the test sample placed over the sample port. The photomultiplier voltage is turned on and the meter reading recorded. The ratio of the sample reading to the standard reading, multiplied by the absolute reflectance of the standard, gives the absolute reflectance of the sample.

This method of measuring reflectance is known as the *substitution method;* the *comparison method* requires an additional port in the sphere for the reflectance standard.

EVALUATION OF THE ERRORS OF THE INTEGRATING SPHERE

To evaluate critically the errors in the integrating sphere, it is necessary to consider the following quantities:

1. The diameter of the sphere, $d_s = 6.00$ in.;

2. The diameter of the sample port, $d_p = 0.75$ in.;

3. The diameter of the light port, $d_L = 0.75$ in.;

4. The diameter of the detector port, $d_0 = 1.00$ in.;

5. The diameter of the aperture stop in the light source as imaged on the sample port, $d_{AI} = 0.36$ in. (for an aperture stop of 0.125 in. diameter);

6. The angular displacement of the optic axis of the light source from the radius through the center of the sample port, $\theta_L = 7.5°$;

7. The reflectance of the sphere coating, R_s varies with wavelength (as shown in Figure 8): at 0.5μ the reflectance is 0.95 and a flat maximum of 0.96 extends from 0.6 to 0.7μ;

8. The goniometric reflection characteristics and absolute reflectance values of the sample and reference, which indicate roughly whether the sample and reference are diffusely or specularly reflecting.

A definitive treatment of the theory of the integrating sphere has been given by Jacquez and Kuppenheim (Reference 7). Their formula for the reflectance ratio of a "perfect" sphere (that is, a sphere in which the test samples, the reflectance standards, and the detector surface, are curved so as to match perfectly the inner surface of the spheres over their appropriate apertures) is:

$$\frac{B_S}{B_{ST}} = \frac{R_S}{R_{ST}} \left[1 - \frac{\frac{(R_{ST} - R_S)\,C}{S}}{1 - \frac{RD}{S} - \frac{R_S C}{S}} \right] \tag{1}$$

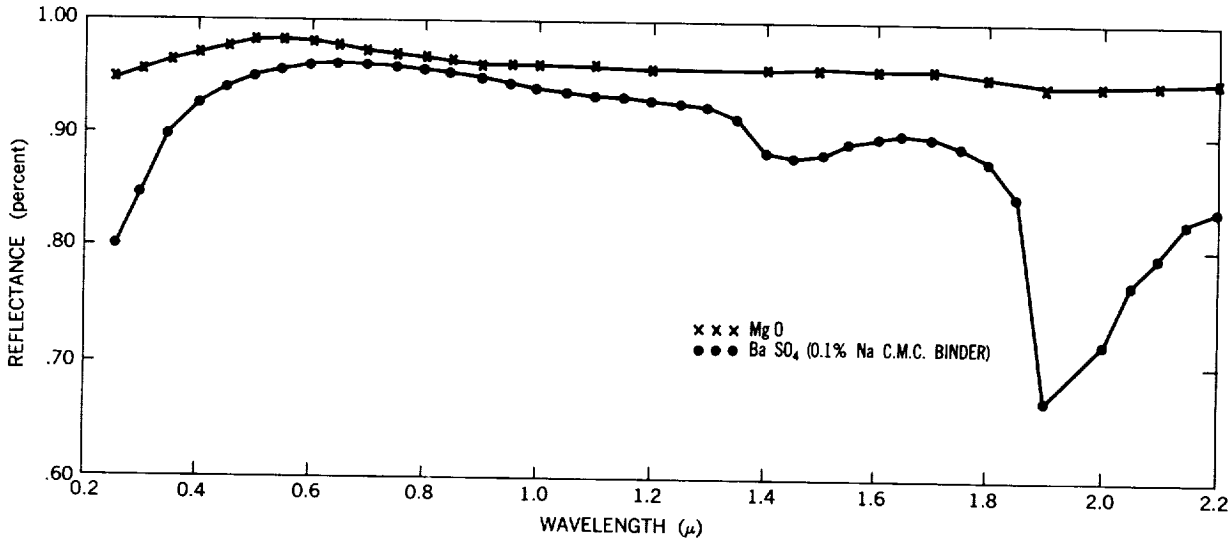

Figure 8—Reflectance of MgO, and $BaSO_4$ (0.1% Na CMC binder), versus wavelength (data from Reference 4).

where

B_S = total light flux passing into the detector port when the test sample is over the sample port,

B_{ST} = total light flux passing into the detector port when the reflectance standard is over the sample port,

R_S = reflectance of the test sample,

R_{ST} = reflectance of the reflectance standard,

R = reflectance of the interior of the integrating sphere,

A = spherical area of the entrance port,

B = spherical area of the photocell port,

C = spherical area of the sample port,

S = total internal area of the sphere, $4\pi R^2$, and

D = S-A-B-C.

Strictly considered, the above formula is not correct for computing the measurement error of flat samples; as Jacquez and Kuppenheim show; however, the formula does indicate the approximate value of the error and is less complex than the correct expression

$$\frac{B_S}{B_{ST}} = \frac{R_S}{R_{ST}}\left[1 - \frac{\frac{(R_{ST} - R_S)RD'C}{S\pi}}{1 - \frac{RD}{S} - \frac{R_S RD'C}{S\pi}}\right], \tag{2}$$

where

$$D' = \int_D \frac{(\rho - L\cos\theta)(L - \rho\cos\theta)}{(\rho^2 + L^2 - 2\rho L\cos\theta)^2}\, da, \tag{3}$$

and θ is the angle between the radius vector of surface integration and the radius through the center of the test sample; ρ, the radius of sphere; L, the distance from center of sphere to center of sample; and da, the element of surface area.

It can be seen from Equation 1 that, for given C, D, S, and R, with R_S and R_{ST} as variables, the maximum value of the error occurs for $R_S = 0$ and $R_{ST} = 1.00$. By evaluating C/S and D/S for the above dimensions, we have $C/S = 0.0039$, and $D/S = 0.985$.

Thus Equation 1 reduces to

$$\frac{B_S}{B_{ST}} = \frac{R_S}{R_{ST}}\left[1 - \frac{0.0039(R_{ST} - R_S)}{1 - 0.985R - .0039R_S}\right]. \tag{4}$$

Equation 4 is applied to the following cases:

1. Aluminum standard, gold sample, 0.35 to 0.90μ;
2. Gold standard, aluminum sample, 0.35 to 0.90μ;
3. 100 percent reflectance standard, black paint (carbon black pigment in a silicon vehicle) sample;
4. 100 percent reflectance standard, white paint (ZnS pigment in a silicon vehicle) sample; and
5. 100 percent reflectance standard, 0 percent reflectance sample.

These results are displayed in Figure 9. (In the above calculations, the sphere wall reflectance was taken from the data presented in Figure 8.) It is seen that the maximum proportional error occurs with the 100 percent reflectance standard and the 0 percent reflectance sample, for which the error is only 7 percent at 6000A.

It should be particularly noted that Equation 1 only applies to perfectly diffuse samples and standards. If the sample is specular and the standard is diffuse, then

$$\frac{B_S}{B_{ST}} \approx \frac{R R_S}{R_{ST}} . \qquad (5)$$

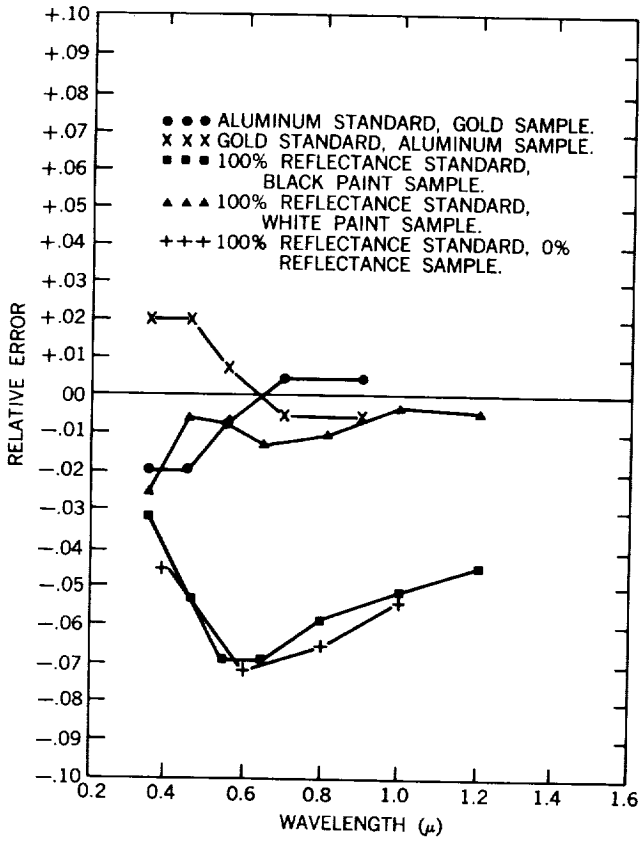

Figure 9—Proportional errors of the perfect integrating sphere for several standard sample combinations. Paint reflectance values are from unpublished data.

If both sample and standard are specular, then $B_S/B_{ST} \approx R_S/R_{ST}$ as in the diffuse case. It is felt that the mathematical expression for the flux ratio of standard to sample for the specular case should yield results similar to those calculated from Equation 1.

The minimum radius of sample curvature which the integrating sphere will measure accurately depends on three factors. These factors are as follows (the numbers refer to the items on page 8):

6. The displacement of the optic axis of the light source from the radius through the center of the sample port, $\theta_L = 7.5°$;
3. The diameter of the light port, $d_L = 0.75$ in.; and
5. The diameter of the aperture stop as imaged at the sample port, $d_{AI} = 0.36$ in. (for a 0.125 in. diameter aperture).

Figure 10 shows the appropriate geometry to be considered in calculating the minimum

radius of sample curvature. At the minimum radius of curvature, a ray from the left edge of the light port A strikes the sample at the right side of the aperture stop image E *normally*. (Actually, only the *effective* light port diameter should be used. This is the diameter of the area of the lens illuminated by the lamp. The size of this illuminated area, in turn, depends on the diameter of the aperture stop, the size of the lamp filament, the aperture-filament and lens-aperture distances, and the relative aperture of a collector lens, if used. For the optical system used in the present integrating sphere, a 0.125 in. diameter aperture would illuminate about half the diameter of the lens). Since the ray AE does strike the sample normally, this means that the reflected ray coincides with AE and that the radius from G to E, GE, is parallel to AE. Using the geometrical relationship between the sides of the approximately similar triangles GEF and GAI, it is found that

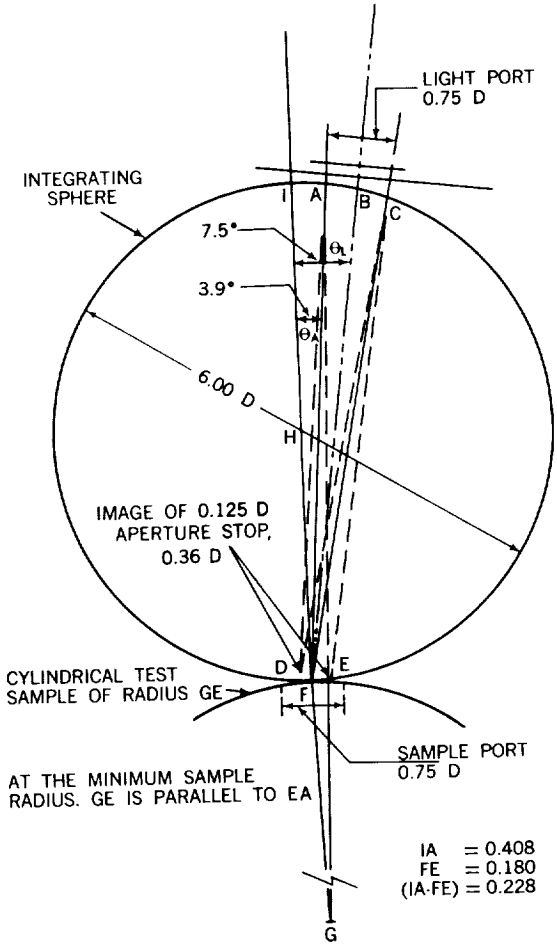

Figure 10—Sphere geometry and the minimum radius of sample curvature with all dimensions in inches.

$$\frac{GE}{FE} \approx \frac{GA}{IA}$$

or

$$GE \approx \frac{FE\ (GE + AE)}{IA}$$

or

$$GE \approx \frac{FE \cdot AE}{IA - FE} \cdot \tag{6}$$

By using the dimensions given in Figure 10, Equation 6 becomes

$$GE \approx \frac{0.180 \times 6.00}{0.228}$$

$$\approx 4.74 \text{ in.}$$

However, as previously mentioned, the full diameter of the light port is not utilized with the 0.125 in. aperture; and, taking 0.375 in. as the approximate effective diameter of the light port, the minimum sample radius of curvature for this situation is found to be GE′ = 2.60 in.

To check this calculation, gold plated cylindrical shells having radii of 3.5, 6.5, 12.5, and 18.5, and 24.5 in. were made up and their reflectance measured with the integrating sphere. The results showed no apparent trend from large to small radii and a variation from the sample mean of ± 1.75 percent, which could quite possibly be due to variation in reflectance of the gold plating from sample to sample.

CONCLUSIONS

It is concluded that the present integrating sphere reflectometer described above is moderately satisfactory for checking the solar absorptance of spacecraft coatings. Desirable future modifications are:

1. A collector lens between the lamp and the aperture stop to increase the light gathering efficiency of the optical system
2. A more stable photomultiplier power supply and amplifier
3. The use of an output recorder
4. An exact analysis of the efficiency of an integrating sphere when used with non-perfectly-diffuse samples and standards
5. Quartz optics to extend the ultraviolet range
6. Attachment of a lightweight monochromator to provide continuous wavelength coverage.

REFERENCES

1. Haas, G., Drummeter, L. F., and Schach, M., "Temperature Stabilization of Highly Reflecting Spherical Satellites," *J. Opt. Soc. Amer.* 49(9):918-924, September 1959.
2. American Institute of Physics Handbook. McGraw-Hill Book Co., Inc., New York, 1957, Section 6, p. 108.
3. Johnson, F. S., "The Solar Constant," *J. Meteorol.* 11(6):431-439, December 1954.
4. Middleton, W. E. K., and Sanders, C. L., "An Improved Sphere Paint," *Illuminating Engineering* 48(5):254-256, May 1953.
5. Jerozal, F. A., "Report on Coatings Monitor," NASA-GSFC, Internal Document No. I 633-62-6, April 9, 1962.
6. Middleton, W. E. K., and Sanders, C. L., "The Absolute Spectral Diffuse Reflectance of Magnesium Oxide," *J. Opt. Soc. Amer.* 41(6):419-424, June 1951.
7. Jacquez, J. A., and Kuppenheim, H. F., "Theory of the Integrating Sphere," *J. Opt. Soc. Amer.* 45(6):460-470, June 1955.

G-294 NASA-Langley, 1963